LEVEL Ⅱ

ARTEC A
ASSOCIATES·INC

79 05 18 004

LEVEL II

⑫

AD A068873

⑥
SHOCK PHYSICS OF
NONIDEAL PLASMAS .

⑭ AR-
Annual Report 13ø

⑪
3ø April 1979

⑨ Final Report. 15 March 1978 to
14 April 1979,

⑫ 64 p.

DDC FILE COPY

DDC
RECEIVED
MAY 23 1979
D

4ø8296

SECURITY CLASSIFICATION OF THIS PAGE (When Data Entered)

REPORT DOCUMENTATION PAGE		READ INSTRUCTIONS BEFORE COMPLETING FORM
1. REPORT NUMBER AR-130	2. GOVT ACCESSION NO.	3. RECIPIENT'S CATALOG NUMBER
4. TITLE (and Subtitle) SHOCK PHYSICS OF NONIDEAL PLASMAS		5. TYPE OF REPORT & PERIOD COVERED Annual Report 15 Mar 78 to 14 Jan 79
		6. PERFORMING ORG. REPORT NUMBER
7. AUTHOR(s) Dennis W. Baum, Stephen P. Gill, W. Lee Shimmin, D. Mukherjee, Robert F. Flagg, and John D. Watson		8. CONTRACT OR GRANT NUMBER(s) N00014-78-C-0354
9. PERFORMING ORGANIZATION NAME AND ADDRESS ARTEC ASSOCIATES INCORPORATED 26046 Eden Landing Road Hayward, California 94545		10. PROGRAM ELEMENT, PROJECT, TASK AREA & WORK UNIT NUMBERS 122401
11. CONTROLLING OFFICE NAME AND ADDRESS Office of Naval Research, Dept. of Navy 800 N. Quincy Street Arlington, Virginia 22217		12. REPORT DATE 30 April 1979
		13. NUMBER OF PAGES 63
14. MONITORING AGENCY NAME & ADDRESS(if different from Controlling Office)		15. SECURITY CLASS. (of this report) UNCLASSIFIED
		15a. DECLASSIFICATION/DOWNGRADING SCHEDULE

16. DISTRIBUTION STATEMENT (of this Report)

Approved for Public Release;
Distribution Unlimited

17. DISTRIBUTION STATEMENT (of the abstract entered in Block 20, if different from Report)

18. SUPPLEMENTARY NOTES

19. KEY WORDS (Continue on reverse side if necessary and identify by block number)

Pulse Power Generation
Explosive Magnetohydrodynamic Generator
High Density Plasmas

20. ABSTRACT (Continue on reverse side if necessary and identify by block number)

This study is an experimental investigation of nonideal plasmas produced by strong shock waves. The study centered about the understanding of factors controlling the specific energy and transport properties of dense plasma in an explosively energized plasma source. The study addressed specifically the gas cavity geometry, pressure-density effects, radial velocity effects, and size scaling. Both argon and xenon were →

DD FORM 1473 EDITION OF 1 NOV 65 IS OBSOLETE

-2- SECURITY CLASSIFICATION OF THIS PAGE (When Data Entered)

DD Form 1473: Report Documentation Page

20. ABSTRACT (Continued)

used for the working gas. Shock speeds ranged from 25.9 to 32.5 km/sec, and measured gas conductivities of 10 to 50 kilosiemens/meter were obtained. The highest peak field amplification in the four shot series was 19 dB.

-3-   UNCLASSIFIED

PREFACE

TABLE OF CONTENTS

LIST OF FIGURES

LIST OF FIGURES (Continued)

LIST OF TABLES

1. INTRODUCTION

This annual report covers research concerned with increasing our understanding of nonideal dense plasmas produced by strong explosively driven shock waves. The research effort was performed for the Office of Naval Research-Power Program under Contract N000014-78-C-0354, and utilized a novel, high performance explosively driven plasma source.

The plasma conditions produced by these new sources are substantially more energetic and nonideal than those investigated or achieved in earlier programs, and underscore the dearth of knowledge and understanding of dense nonideal plasmas.

The research effort covered in this report consists mainly of four explosively driven plasma source experiments that were designed, fabricated, instrumented, fired, and analyzed during the course of this contract period.

1.1 Background

For several years Artec Associates has been actively engaged in pulsed power generation using an explosively driven MHD concept[1,2,3]. The key element of this novel concept is a plasma source which converts the chemical

energy of an explosive into a very high enthalpy fully
ionized plasma. The high density plasma is in turn driven
into a channel and through a magnetic field in a MHD section.
The electrical output of this section is used to power an
augmenting magnetic field intensifying the total magnetic
field through self-excitation and ultimately driving an
external load.

The concept of a fully self-excited explosive MHD
pulse power generator is particularly attractive for many
Naval applications. Such a generator, consisting only of
explosive, metal tubing and a permanent magnet, would have
an attractively long shelf-life. Startup time from initia-
tion to full power is nearly instantaneous, and tens of
megajoules of electrical energy are available at gigawatt
power levels. These explosive generators are inherently
small, and compatible with many special weapon applications.
Other applications may well become apparent as the program
progresses.

Explosive MHD generators of the externally-excited
variety have been experimentally demonstrated many times
in the past, but the real progress toward a fully self-
excited generator has been thwarted by a lack of knowledge
of the properties of dense nonideal plasmas. Measured

electrical conductivities in our experiments for example are substantially less (up to a factor of 10) than calculations based on ideal plasma theory. To compensate for the difference and to still achieve full self-excitation it has been necessary to increase both energy and duration of the explosive plasma source.

1.2 Previous Research Effort

Previous research has been directed toward investigating the shock physics of nonideal plasmas[1], and developing an advanced high-performance plasma source. This effort was quite successful, and Artec Associates conceived an explosive plasma source that was far more energetic than any used before.

The new, high performance explosive plasma source compresses plasma to denser, more nonideal states than before. Much of the energy addition to the plasma occurs at densities exceeding normal solid density for many materials and nonideal effects dominate the plasma behavior.

2. EXPERIMENTAL RESEARCH ON NONIDEAL PLASMAS

2.1 Description of the Plasma Source

A schematic diagram of the plasma source is shown in Figure 1. It is comprised of an annular region of argon gas which is shock-compressed by a detonating explosive. At the end of the cylindrically symmetric annular region, the shocked argon is converged radially into a hemispherical transition section and exhausted into a diagnostic channel located on-axis. This driver configuration was used in three shots, 130-2, 130-3, and 130-4. The conical driver shown in Figure 2 and discussed in previous reports was used to drive Shot 130-1.

The annular portion of the plasma source operates much as the explosive plasma sources described in earlier research reports[1,2,3]. More energy is added to the plasma by the pronounced radial convergence of the flow and explosive compression of the reservoir. In other words, the converging shock flow now stagnates along the axis, forming a much higher pressure, higher density plasma reservoir than previously. Nearly simultaneously, the metal cap at the end of the interior explosive is explosively accelerated and compresses and energizes the plasma even further. As can be appreciated, the convergence, compression, and exhaust processes are all mutually dependent. Timing is critical
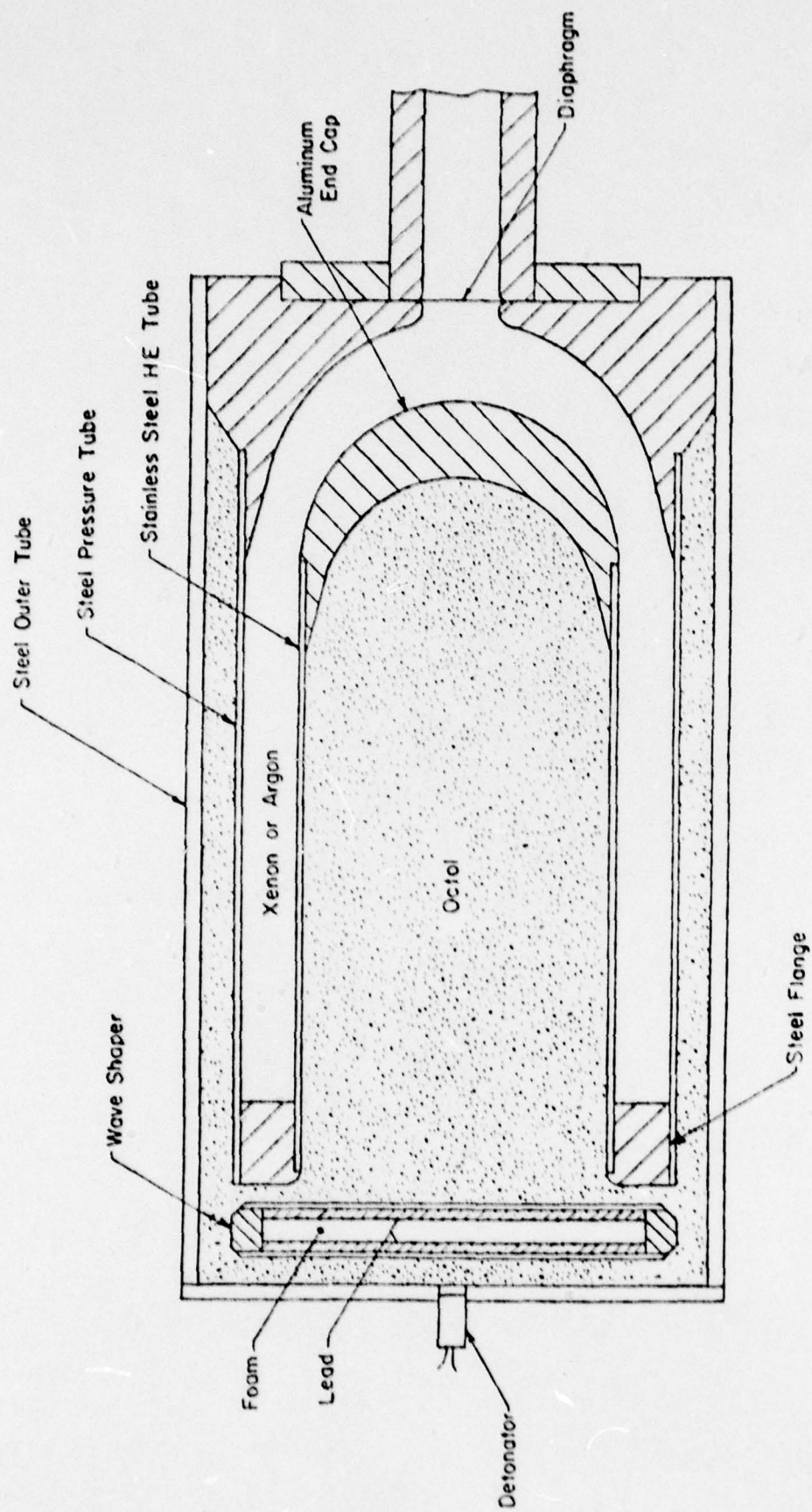
Figure 1 Schematic of Plasma Source for Shots 130-2, 130-3, and 130-4
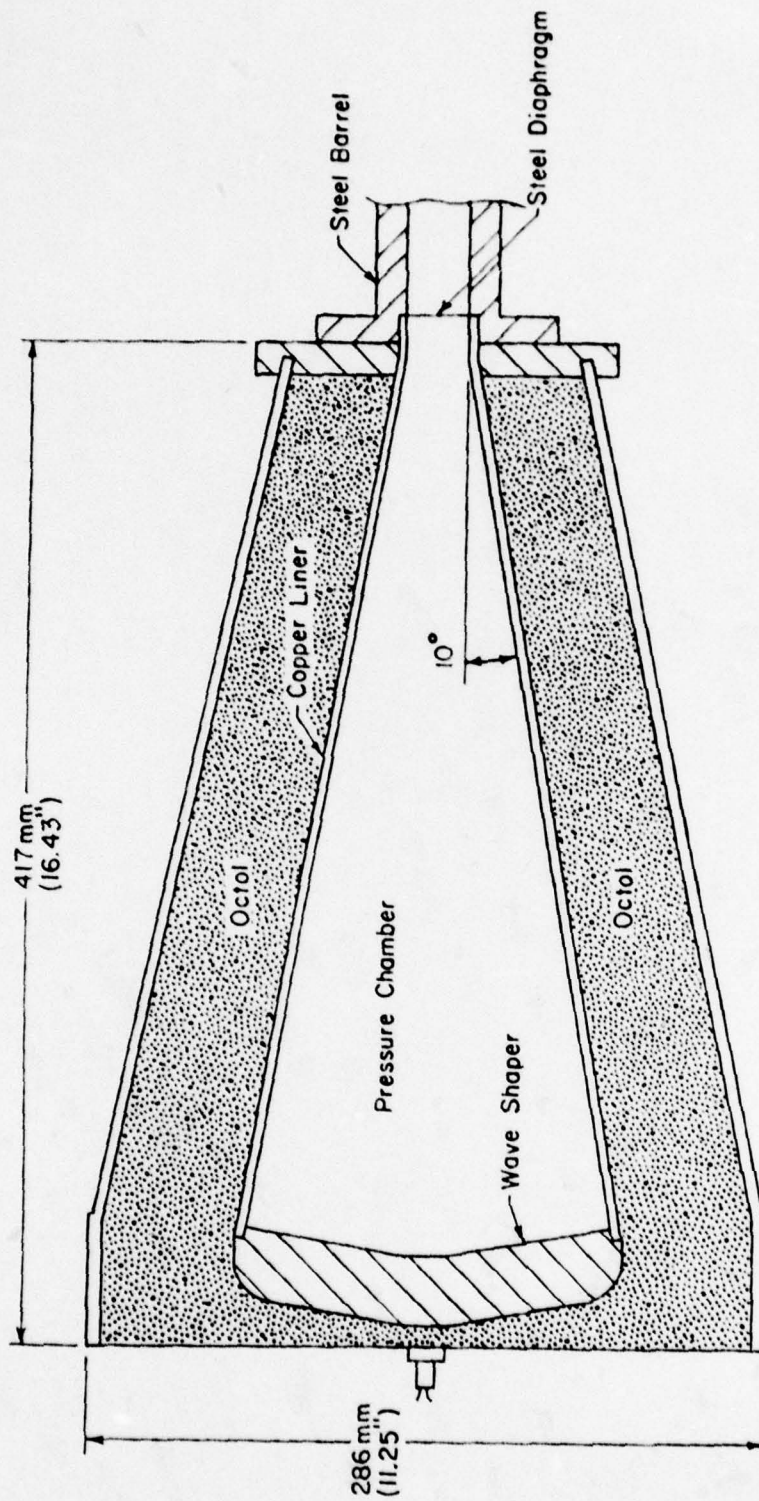
Figure 2 Schematic of Conical Plasma Source for Shot 130-1

-14-

in achieving high performance of the plasma source but
experimental performance of the plasma source has been
very satisfying, even though the design has not yet been
optimized.

Overall efficiency, i.e. conversion of explosive chem-
ical energy to useful plasma enthalpy, already exceeds 25%,
and will most likely be increased further with design re-
finements. We note that plasma energy is higher than that
achieved in any previous plasma source. MHD channel con-
ditions are also very good, and even with a relatively
small diameter driver, a significant degree of generator
self-excitation has been achieved. Full self-excitation
appears highly probable with a larger source, or with
mechanical design refinements.

2.2 Estimate of Nonideal Plasma States

Plasma states achieved in the new plasma source may
be estimated from experimental data and the best available
nonideal plasma theory[4]. The initial driver shock wave in
the annular region of the plasma source has a measured par-
ticle velocity of 8.5 km/s (the detonation velocity of
Octol). Using this measured velocity and assuming the
Debye-Huckel theory with a zero shielding coefficient, the
shocked gas conditions are calculated to be: pressure,

3GPa (30 kbar); density, 0.33 Mg/m^3 (g/cm^3); and energy 37 MJ/kg. These estimates are fairly accurate, as the pressure and energy states behind a shock are relatively insensitive to uncertainties in the equation of state. However, the Debye-Huckel plasma theory used in the calculations is about at the limit of credibility because of the dense plasma state.

An estimate of the reservoir entropy state may be calculated assuming a single strong reflected shock. To account for the high density, we have used the empirical Jones-Wilkins-Lee (JWL)[5],[6] equation of state commonly used in explosive detonation theory. Calculated conditions for the above initial shock are: pressure, 35 GPa (350 kbar); density, 1.30 Mg/m^3 (g/cm^3); and energy, 80 MJ/kg.

Final compressed state in the reservoir can be estimated assuming an isentropic compression of this stagnated region to a value obtained by matching experimental shock velocity data. For example, the magnitude of the shock velocity in the diagnostic channel is a direct consequence of specific reservoir conditions. By matching the experimental data for shock velocity, a unique value of the reservoir conditions can be obtained. Using this approach, peak plasma conditions in the reservoir were determined to be: pressure,

84 GPa (840 kbar): density, 2.2 Mg/m^3 (g/cm^3); and energy
97 MJ/kg.

Plasma states in the reservoir achieved by the new
plasma source are located almost off the edge of the plasma
parameter chart, shown in Figure 3, and even the expanded
plasma is well into the nonideal region at the right of
the plasma parameter chart. The chart and the parameters
were described previously in our 1978 research report[1],
but key parts will be summarized here. QNTM is the ratio
of electron thermal deBroglie wavelength to Debye length.
For values greater than 0.1 quantum diffraction effects
become important in plasma theory. INTPAR is the plasma
nonideal interaction parameter, i.e. the ratio of coulomb
electrostatic energy to thermal kinetic energy. Ideal
plasma theory assumes INTPAR to be very small. In fact
the Debye-Huckel theory, which represents a first order
correction to ideal plasma theory, is known to be invalid
above an interaction parameter of 0.47. Finally, DGN is
the quantum degeneracy parameter, the ratio between electron
thermal deBroglie wavelength to electron separation.

It can be seen from the figure that the Artec plasma
source yields conditions well into the nonideal plasma
regime, indeed much further than the earlier plasma sources.
In order to understand the details of the shock energization
process, particularly the final compression of the reservoir,

Fig. 3   Plasma Parameter Chart for Argon
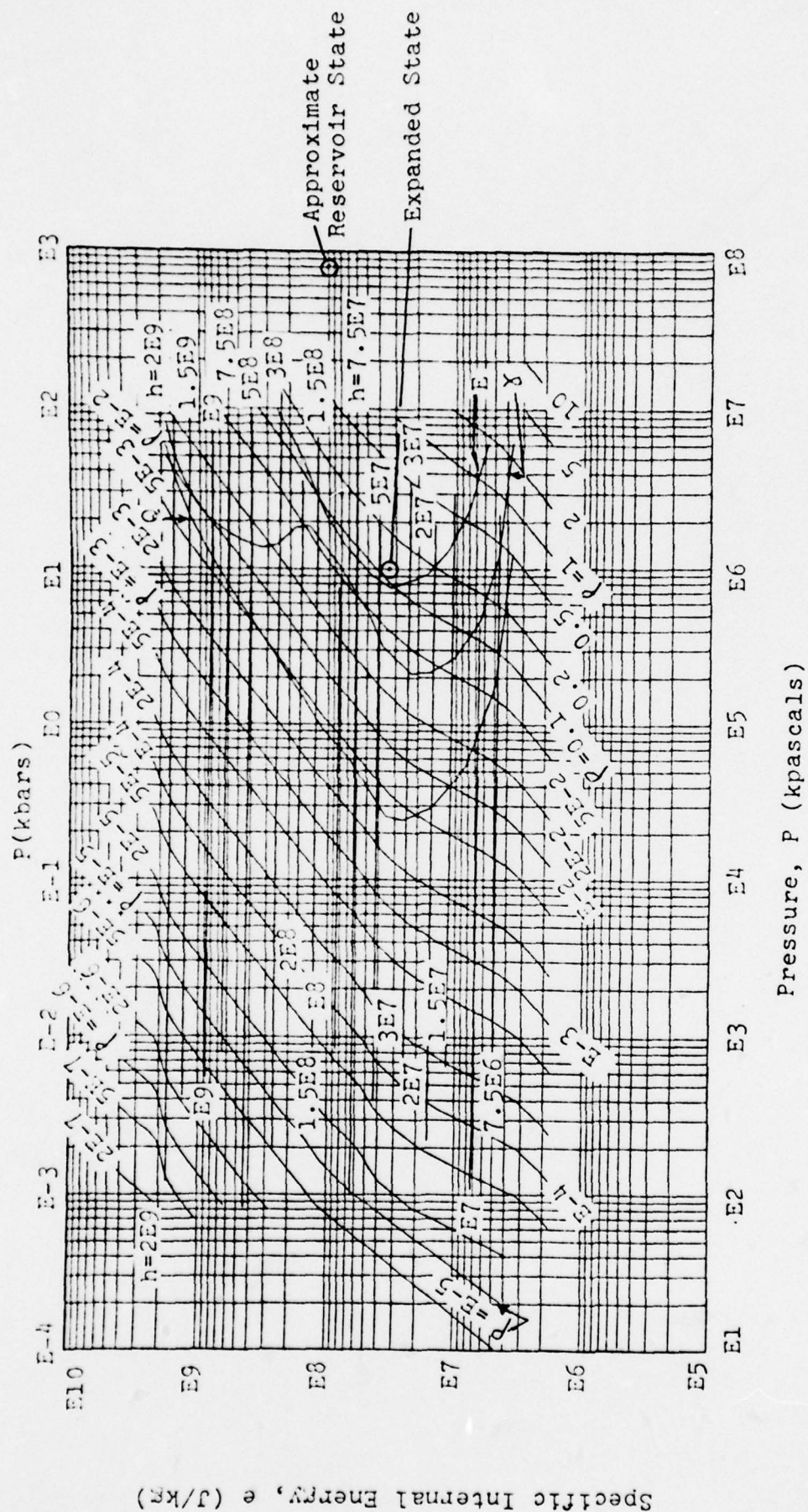
it is necessary to have a clear understanding of the physics
of strongly nonideal plasmas. Once the plasma expands into
the MHD channel, the static pressures drop to about 0.1 GPa
(1 kbar), hence the MHD interaction process can be studied
using "moderately nonideal" plasma theory.

2.3 Description of the Experimental Apparatus

Four experiments were designed, instrumented and fielded
for this contract. The basic design parameters are given in
Table 1.

Shot 130-1 utilized a conical driver and xenon gas at
137 kilopascals (20 psia) as the driver gas. The main
purpose of this experiment was to fire a conical imploding
driver, measure the flow properties of the driver gas as it
expanded into a partially evacuated channel, and compare
these properties with the expected flow properties based
on calculated driver performance.

Shot 130-2 utilized a 17 cm diameter imploding/exploding
driver with xenon gas at 694 kilopascals (100 psia) as the
driver gas. The main purposes of this experiment were to
evaluate this type of driver, to measure the properties of
the plasma as it expanded into a partially evacuated channel,

TABLE 1 PLASMA SOURCE PARAMETERS

Shot No.	Plasma Source	Source Diameter	Driver Gas	Initial Pressure in Channel	Explosive	Shock Pressure
130-1	Conical	17 cm	20 grams Xenon	6.65 Kpascals	75/25 Octol	30 Kbars
130-2	Annular	17 cm	55 grams Xenon	6.65 Kilo-pascals	75/25 Octol	30 Kbars
130-3	Annular	17 cm	55 grams Argon	6.65 Kilo-pascals	75/25 Octol	30 Kbars
130-4	Annular	30 cm	302 grams Argon	6.65 Kilo-pascals	75/25 Octol	30 Kbars

and to assess the improvement in performance of this source by comparing the output with the configuration of Shot 130-1.

Shot 130-3 utilized a 17 cm. diameter imploding/exploding driver as before but with argon at 2.12 megapascals as the driver gas. The purpose of this experiment was to fire an imploding/exploding type plasma source using argon and compare the resulting performance with the same configuration using xenon (Shot 130-2). Plasma output was to be assessed using the same diagnostics as Shot 130-2, and in addition a self-excited MHD station was included for additional diagnosis of the plasma parameters.

Shot 130-4 utilized a 30 cm. imploding/exploding driver with argon at 2.07 megapascals as the driver gas. It was felt that the mass of the driver-processed-gas in the 17 cm. diameter drivers was limiting the flow duration of the channel flow to nominally 30 microseconds, and that increasing the outside diameter to 30 centimeters and the mass of the gas by better than fivefold would increase the total flow time to 50 to 60 microseconds, and permit as much as 40 dB magnetic field enhancement.

Additionally, a minor redesign of the field coil to prevent mechanical short circuits was also included on 130-4

to negate suspected shorts which we initially suspected
helped to limit the increase in magnetic field in 130-3
to 19 dB.

2.4 Description of the Diagnostics

Shot 130-1: A drawing of the plasma source used in
this shot was shown previously in Figure 2. The explosive
used was 75/25 Octol; the imploding liner was copper (4.0 mm.
or 156 mils thick); the cone half-angle was 10^0; and the
charge-to-mass ratio was 3.9. The thick steel wave shaper
permitted a single detonator to provide a symmetrical annular
detonation front. The cone angle was calculated to produce
an axially progressing impact point with a speed of 17 km/s.

The driver gas chamber was loaded with 20 grams of
xenon to provide a nominal shock pressure of 2.4 GPa (24
kbar). The diagnostic channel was loaded with air at 6.65
kPa (50 Torr) and was separated from the driver by a thin
steel diaphragm.

The layout of the diagnostics in the channel is shown
in Figure 4. There was one velocity gage or open circuit
voltage measurement and one electrode station with an 11
milliohm load (a thin strip of stainless steel) at which
the loaded voltage and current were to be measured. A pair

Barium Ferrite Magnet

Conductivity Gage No.1

Conductivity Gage No. 2

Top View

Velocity Gage

Load

Side View
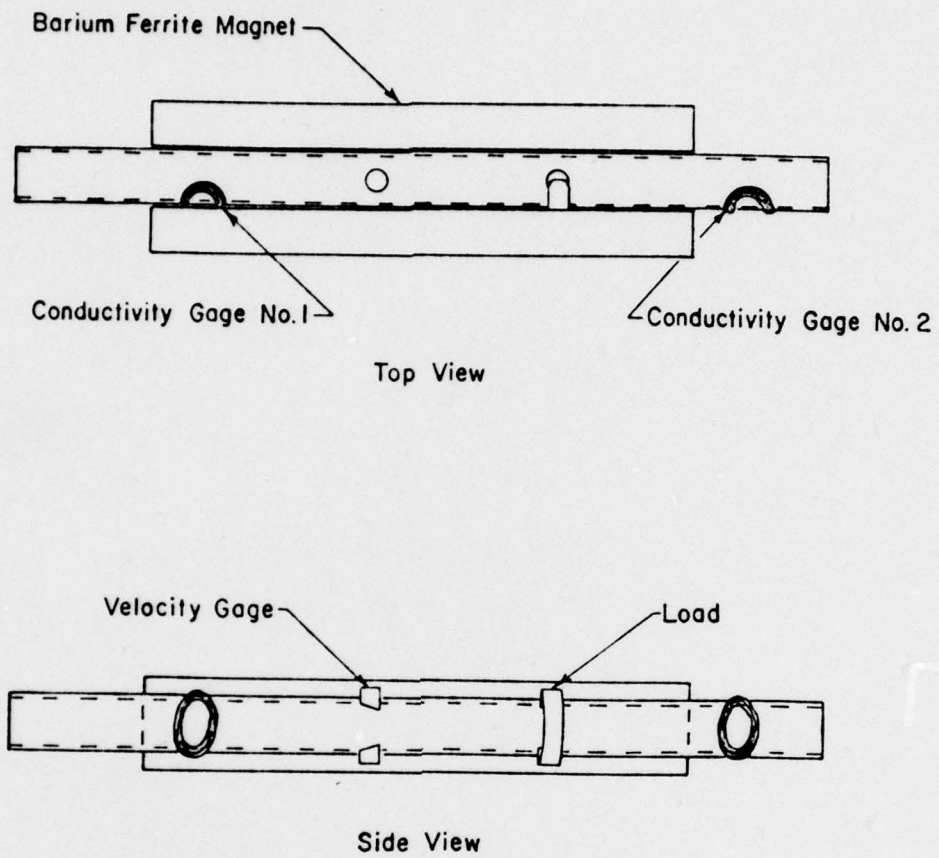
Figure 4   Layout of Diagnostics for Shots 130-1 and 130-2

of 0.3 meter-long barium-ferrite magnets provided a transverse magnetic field of 77 mT (770 gauss) and 83 mT (830 gauss) at the velocity gage and load stations respectively. There were two conductivity gages, one located near the upstream end of the magnets and one near the downstream end as shown in the figure.

Shot 130-2: A drawing of the plasma source was shown previously in Figure 1. The explosive used was 75/25 Octol. The wave shaper was so configured that a single detonator on-axis provided a symmetric detonation front sweeping along both tubes simultaneously.

The driver gas chamber was loaded with 56 grams of xenon to provide a nominal shock pressure of 3.0 GPa (30 kbar). The diagnostic channel was loaded with air at 6.65 kPa (50 Torr) and was separated from the driver by a 25μm thick stainless steel diaphragm.

The layout of the diagnostics in the channel is shown in Figure 4 and is identical with Shot 130-1. There was one velocity gage or open circuit voltage measurement and one electrode station with an 11 milliohm load (a thin strip of stainless steel) at which the loaded voltage and current were measured. A pair of 0.3 meter-long barium-ferrite magnets provided a transverse magnetic field of

-24-

75 mT (760 gauss) and 89 mT (890 gauss) at the velocity
gage and load stations respectively. There were two con-
ductivity gages, one located near the upstream end of the
magnets and one near the downstream end as shown in the
figure.

Shot 130-3: The mechanical configuration of the
experiment was the same as Shot 130-2, except that the
driver was loaded with argon gas instead of xenon. Nominal
shock pressure in the driver was 3.0 GPa (30 kbar) and the
diagnostic channel was loaded with air at 6.65 kPa (50 Torr).

The first part of the diagnostic channel, comprising
two conductivity gages, a velocity gage, and an MHD load
station, was identical to Shot 130-2. The second part of
the diagnostic channel included a self-excited MHD generator
stage and a third conductivity gage. Experimental layout
of the generator section is shown in Figure 5.

A pair of 150 mm. long barium-ferrite magnets provided
a transverse mangetic field of 82 mT at the generator loca-
tion. Flush brass electrodes, 25 mm. long and 80 degrees
wide (on a 25 mm. diameter channel) were soldered directly
to a one-turn self-excitation coil made from #10 AWG wire
braid. Measured inductance and resistance of the field

Barium Ferrite
Magnet

Generator Volts
From Electrodes

Top View

Braided Field Coil

Conductivity Gage
No. 3

Side View
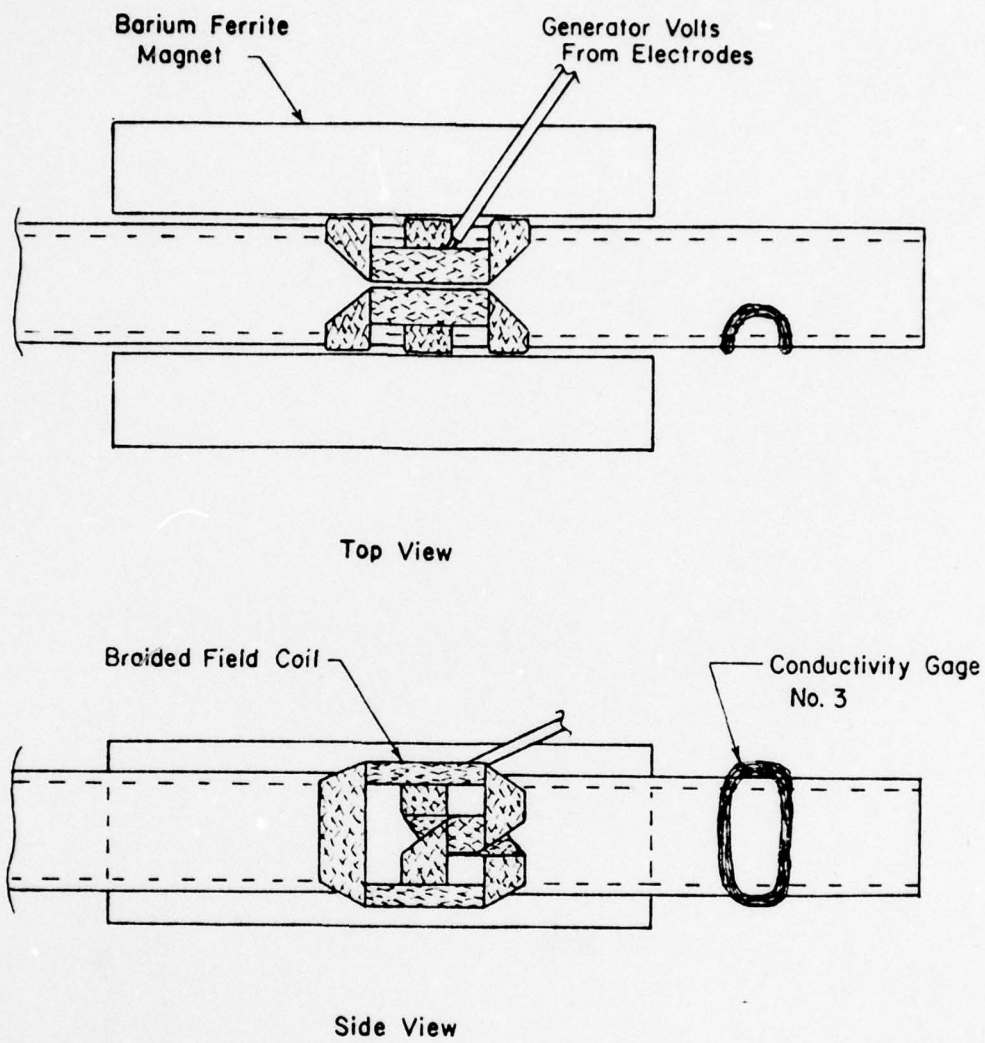
Figure 5   Layout of Self-Excited Generator Station

coil were 35.9 nanohenries and 0.403 milliohms respectively.
Measured B/I ratio at the tube wall was 18.2 microTesla/amp.

Shot 130-4: The geometrical configuration of 130-4
was nearly identical to 130-3 except that the driver outside
diameter was increased to 30 centimeters. A full 2X scale
up from the baseline 17 centimeters was discarded since
tubing of the desired dimensions is not commercially avail-
able. The driver gas was argon and the diagnostic channel
was loaded with air at 6.65 kilopascals (50 Torr) as pre-
viously.

The first section of the diagnostic channel contained
2 side-mounted conductivity gages (gages 1 and 2), a
velocity gage and a conventional MHD generator. The mag-
netic field for these 3 diagnostic tools was provided by
two barium-ferrite permanent magnets mounted to produce a
B field of .09 Tesla orthogonal to the flow velocity vector.

The second section of the diagnostic channel included
a third side-mounted conductivity gage and a self-excited
MHD generator stage. The experimental configuration is
given schematically in Figure 6.

The initial magnetic field for this section was pro-
vided by a pair of barium-ferrite permanent magnets.
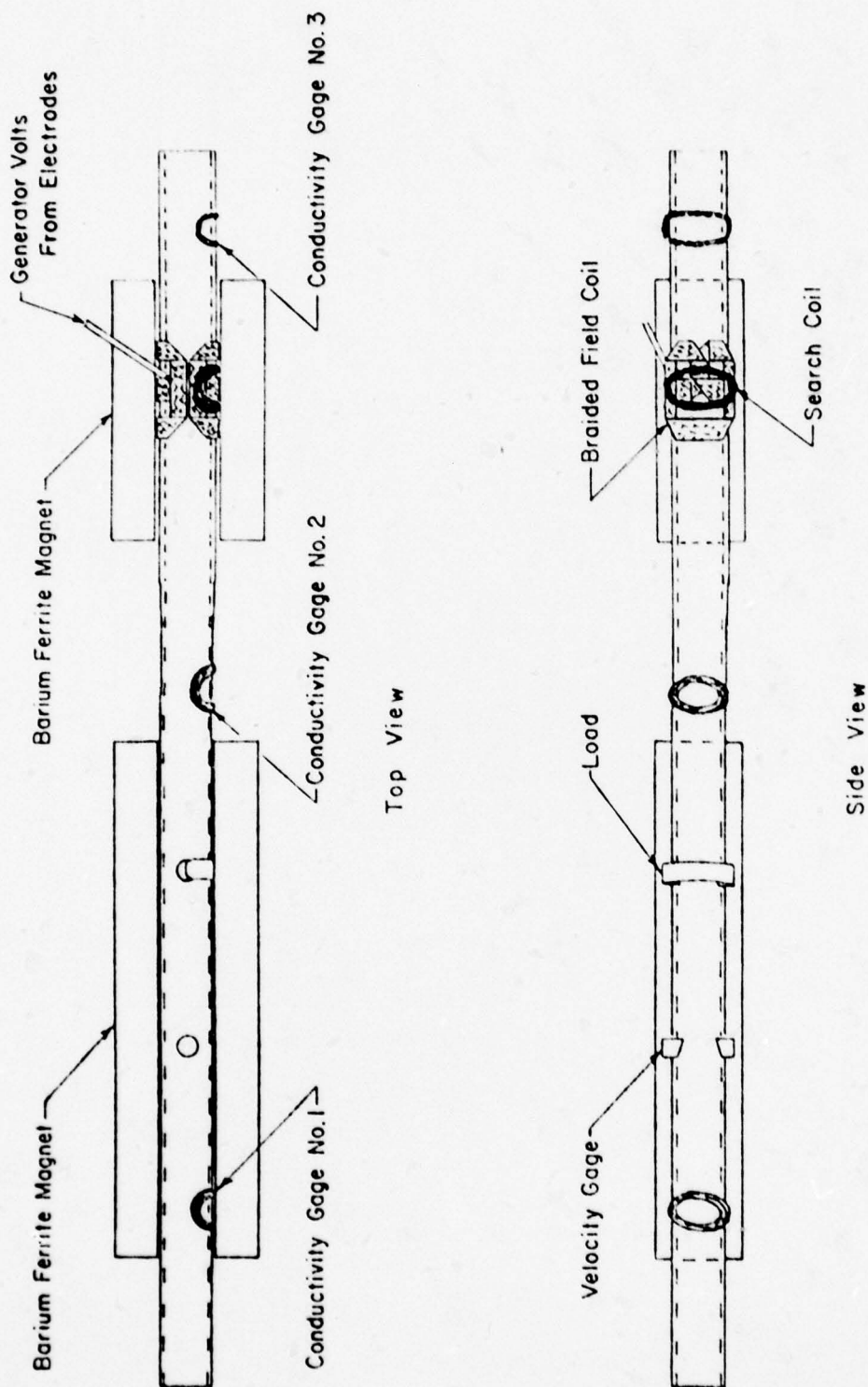
Figure 6 Channel Layout for Shot 130-4

Additionally, flush brass electrodes were connected to a low inductance one-turn self-excitation coil made from #8 AWG wire braid. The measured inductance of the field coil was 37.9 nanohenries. The D.C. resistance was 0.525 milliohms. The measured B/I at the tube centerline was 24.3 microtesla per amp.

3. RESULTS AND CONCLUSIONS

3.1 Plasma Source Performance

Pairs of symmetrical ionization pins placed on either side of the plasma source reported within fractions of a microsecond of each other, verifying the symmetry of the detonation. The pins also verified the correct (expected) detonation velocity for Octol, 8.48 km/sec. A typical plot of driver ionization pin data is shown in Figure 7. The precision and symmetry of the data is clear from the figure.

In all cases the driver gas initial pressure (hence density) was adjusted to yield 30 kbars static pressure behind the driven initial shock. This nominal or standard condition was used in each case to allow comparing the different cases, one with another.

A flash X-ray photograph of an annular plasma source, shown with the detonation wave approximately half way along the driver, is given in Figure 8. The high degree of symmetry both for the inside and outside collapsing walls and from one side to the other is evident.

In the linear section of the source for 130-2 and 130-3, the total enthalpy was 80.2 MJ/kg giving a total energy of 4.5 MJ for the 56 grams of gas. In the convergent section of the source, which effectively acts as a reservoir, the
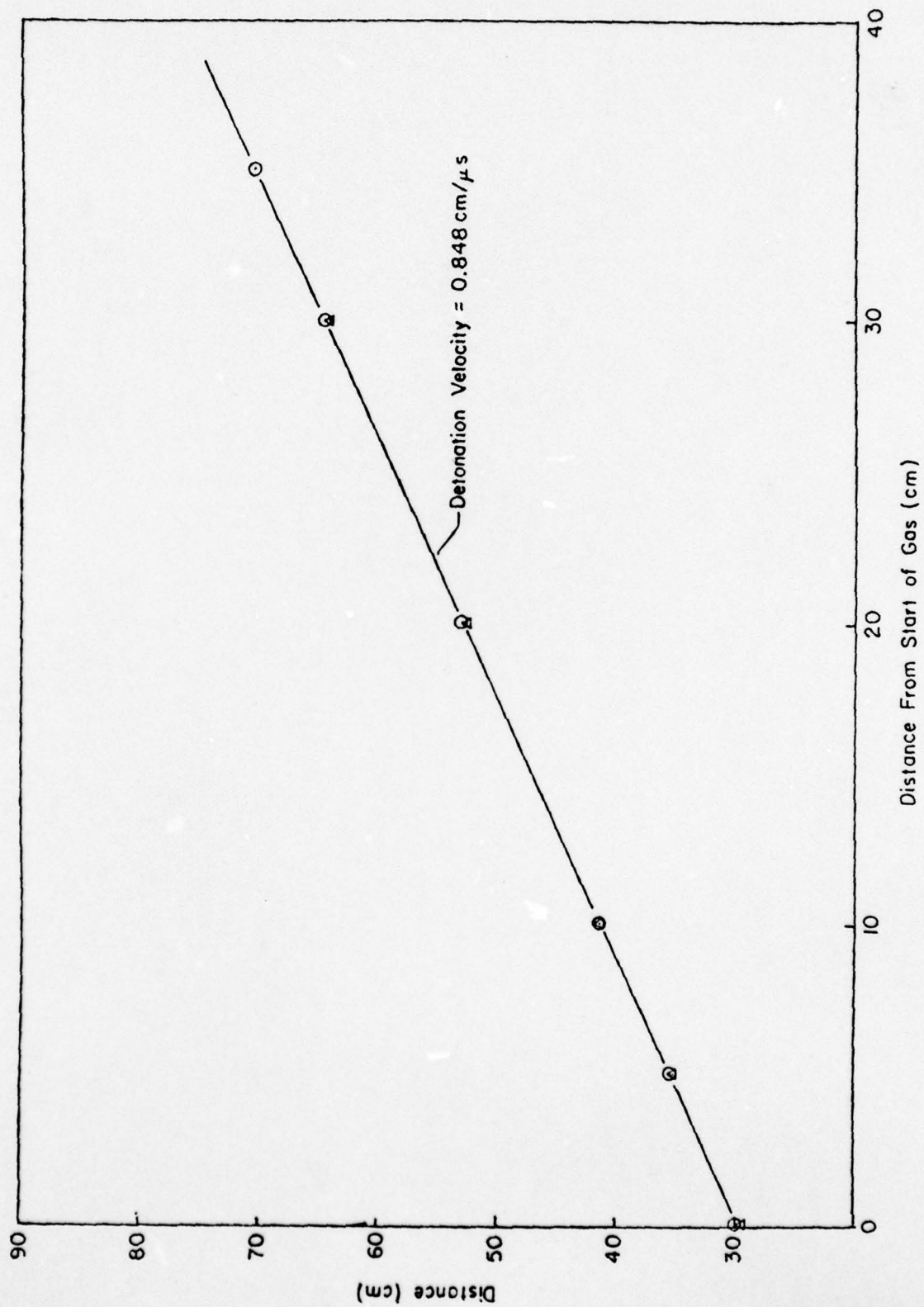
Figure 7 Distance-Time Diagram for Octol Annular Plasma Source (l3O-4)

Distance From Start of Gas (cm)

Detonation Velocity = 0.848 cm/μs

Distance (cm)
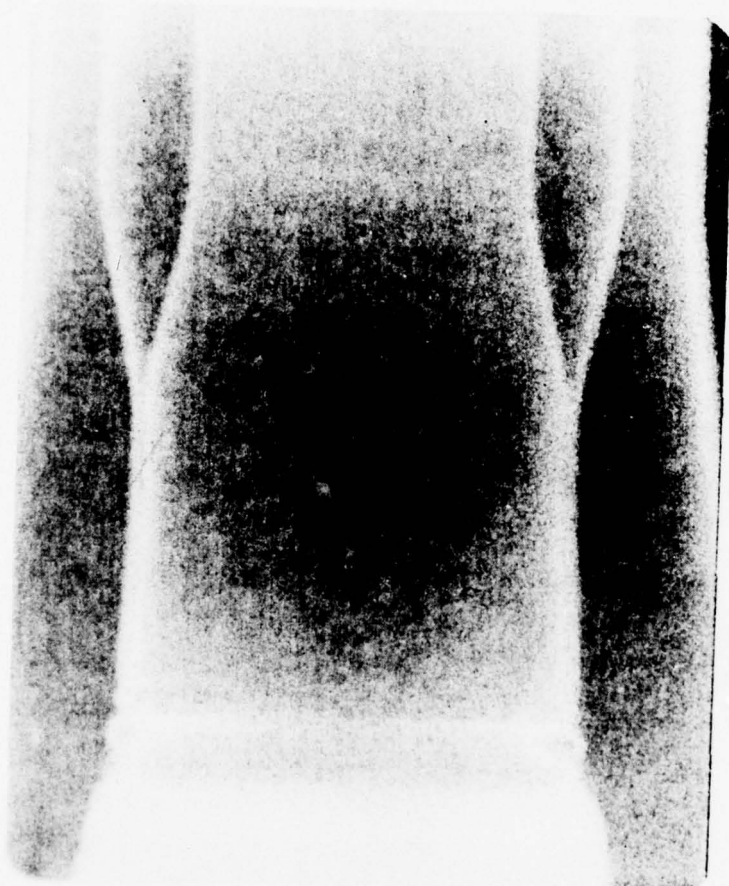
Figure 8   120 MEV Flash Radiograph of a 30 kbar High Efficiency Explosive Plasma Source

total enthalpy is estimated to be 134 MJ/kg. On the assumption that all of the gas achieved this enthalpy, the total energy in the plasma was 7.5 MJ.

3.2 Channel Conditions

The initial pressure in the diagnostic channel in all cases was 6.65 kilopascals (50 Torr) of air, hence the performance of all the sources in terms of the equivalent reservoir conditions produced can be seen from a comparison of the initial shock velocity in the diagnostic channel. These velocities are tabulated in Table 2.

For Shot 130-1, a channel shock speed of 27.3 km/s was obtained from shock front arrival times at the diagnostic stations and from shock breakout at the diaphragm which was monitored by a photodiode. The initial plasma flow velocity calculated from the observed shock velocity is 24.8 km/s. From the velocity gage record the initial flow velocity was measured to be 22.7 km/s, which is 8 percent below the calculated value. Since this particular velocity gage was located five channel diameters downstream of the magnet edge and since the magnetic Reynolds number of the flow was not sufficiently high to cause significant perturbation of the velocity gage reading at that distance, we suspect the source of the discrepancy must lie in other than R_m effects.

TABLE 2   INITIAL SHOCK AND FLOW VELOCITIES

Shot No.	Measured Initial Shock Velocity (km/sec)	Measured Initial Flow Velocity (km/sec)	Calculated Initial Flow Velocity (km/sec)
130-1	27.3	22.7	24.8
130-2	25.9	19.2	23.6
130-3	26.4	20.6	23.6
130-4	32.5	27.3	29.7

For Shot 130-2, a channel shock speed of 25.9 km/s
was obtained from shock front arrival times at the diagnos-
tic stations and from shock breakout at the diaphragm, which
was monitored by a photodiode. This slightly lower velocity
(5 percent compared to the previous shot) is probably within
the experimental scatter in the data.

For Shot 130-3, a channel shock velocity of 26.4 km/s
was measured, compared to 25.9 km/s in the previous shot,
and is essentially the same, implying that, from a shock
velocity point of view, argon and xenon drivers are nearly
identical in performance.

A channel shock velocity of 32.5 km/s was measured
for Shot 130-4 compared to 26.4 km/s and 25.9 km/s for
the previous shots, respectively. Hence it is clear that
the larger driver and its increased convergence of driver
gas produce greater peak reservoir conditions, hence greater
shock velocities at the diagnostic stations. Indeed, this
shock velocity is the highest that has been obtained in
the program to data, and as such represents a milestone in
our progress.

Tabulated in Table 2 are the measured and calculated
initial flow velocities for these four experiments. One

notes generally that the calculated flow velocity and the measured flow velocity differ with the measured values being lower than the calculations by 5-20 percent. This is probably within our ability to infer reservoir conditions at this point in time. The difficulty is threefold; 1, the equation of state for the driver gases at near megabar pressures is not precisely known. 2, calculating the expected flow velocity requires assuming an expansion process from "known" reservoir conditions. As the reservoir conditions are not steady in time, the expansion process is not the simple process modeled in the calculation, i.e. steady flow expansion to the channel entrance where the flow Mach number equals 1 followed by an unsteady flow expansion along the channel. 3, as the expansion processes are not simple, but contain upstream and downstream running shock and rarefaction waves[7], seeking a single representative number for initial shock speed may not be realistic in practice.

The flow velocity histories for the four shots are shown in Figure 9. Four points are worth noting. The conical driver of Shot 130-1 has a slightly higher peak flow velocity than either 130-2 or 130-2, but the decay rate is much greater and the total flow time is less than one-half of that from 130-2 or 3. The argon and xenon shots with the 17 cm. diameter driver produce very similar flow
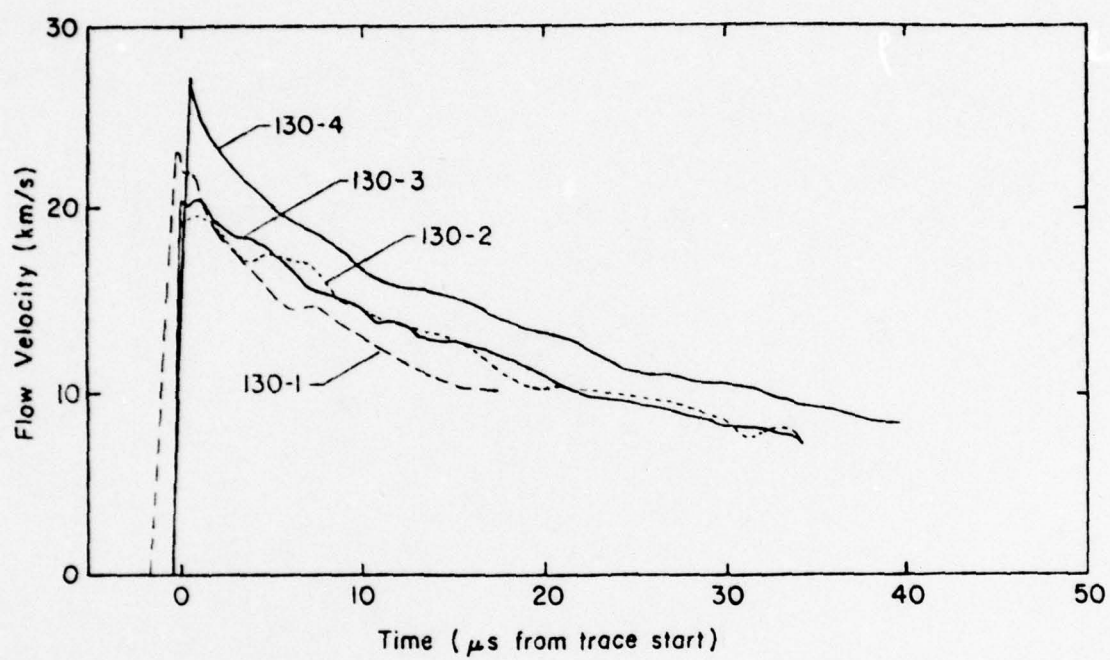
Figure 9 Comparison of Flow Velocities

velocity histories, both in absolute value of velocity and flow time.

The 30 cm. diameter driver of 130-4 gives substantially greater flow velocities; indeed the highest peak obtained in our research to date. These velocities are greater at any given time and are maintained to approximately 40-45 microseconds in time. The efficacy of the larger diameter driver is clearly apparent from this trace. However, the decay of the channel is greater than expected. The decline in velocity implies that the higher reservoir conditions are not being maintained as long as would have been expected with the additional mass of working gas produced by the larger driver.

These points suggest the possibility that other previously unsuspected phenomena may be limiting test flow time both for the small driver as well as the large. A prime candidate is the premature "pinching off" of the flow at the channel entrance by distortions of the entrance region by the very high reservoir pressures. This type of behavior has been observed by others, for example, the computer experiments of the Voitenko compressor performed by Brown and Lohmann of LLL[8]. They observed that at very high reservoir pressures, well in excess of the yield stresses

in the reservoir wall material, the reservoir end wall near the channel is extruded in the channel entrance region, "pinching off" the outflow. Even if the flow is not completely blocked, a "nozzle" is created at the channel entrance requiring the gases expand further in a steady expansion before shifting to an unsteady expansion. As the steady expansion is less efficient in translating pressure into velocity than the unsteady expansion for flow Mach numbers greater than unity, less shock velocity is obtained for a given reservoir condition. A discussion of this subtle but not commonly appreciated point is given in Reference 7.

This problem, and modifications to the reservoir--channel transition area to counter it, will be addressed in future work.

3.3 Expanded Plasma Electrical Properties

The electrical conductivity of the gas in the channel is of key interest in this research. Not only are precise values of conductivity presently impossible to obtain theoretically due to the complex nonideal nature of the plasmas, but the measurements also include significant scatter in results, both from similar instrumentation and between different measurement techniques.

For example, Figure 10 shows electrical conductivity determined from an eddy current gage (described earlier) and that determined from examining the V-I characteristics of the loaded generator section. One notes that the conductivities vary by about a factor of two with the eddy current gage giving the higher values.

The conductivity results from Shot 130-2 are shown in Figure 11. In this case, two electrical conductivity gages were used, one upstream and one downstream of the load section (see Figure 4). The gages gave similar results with the downstream gage giving generally slightly higher values. One also notes that the conductivity histories are maintained in time better than 130-1 as would be expected from examining the particle velocity histories of the two shots.

As previously, one also notes that the values determined from the load section are lower by about 50 percent.

The electrical conductivity data for Shot 130-3 are given in Figure 12. In this shot, 3 eddy current gages were used to obtained conductivity in addition to the values determined from the load resistance, and self-excited generator sections. The locations of the 5 different
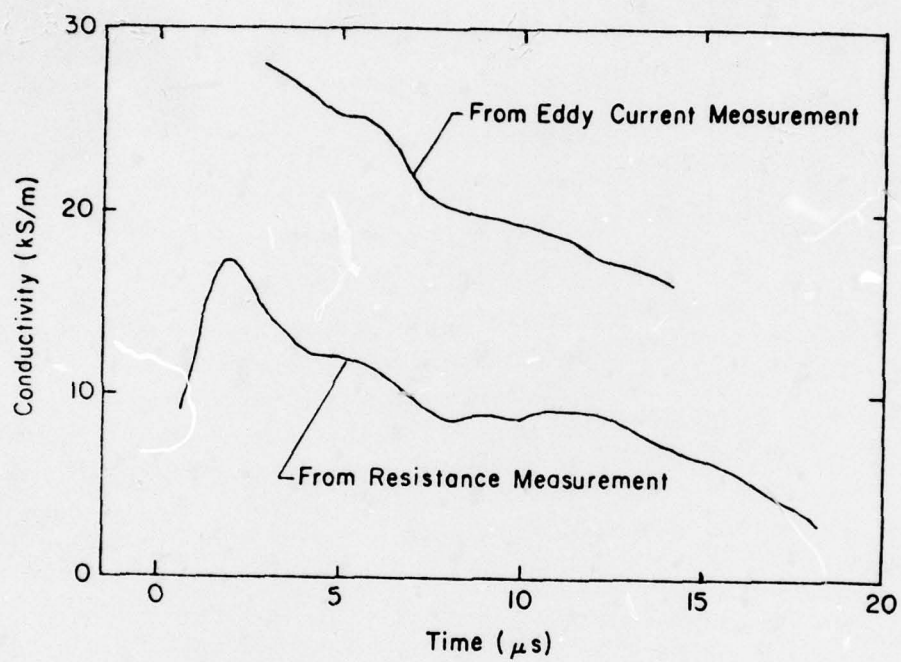
Figure 10 Channel Plasma Conditions Measured on Shot 130-1
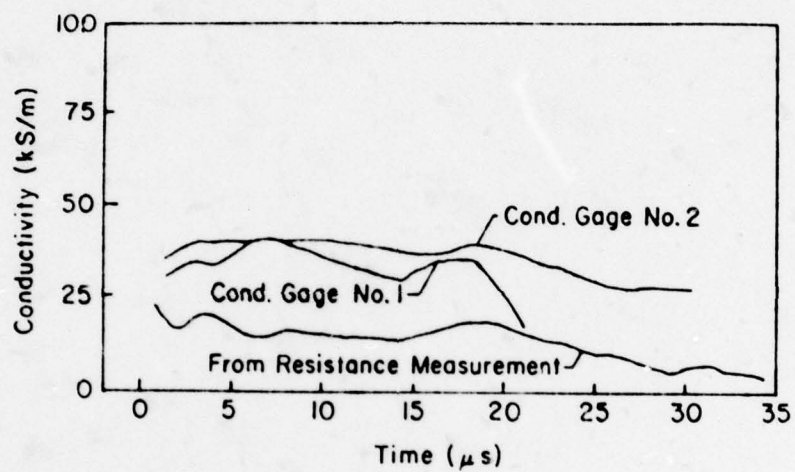
Figure 11 Results of Plasma Properties Measurements on Shot 130-2
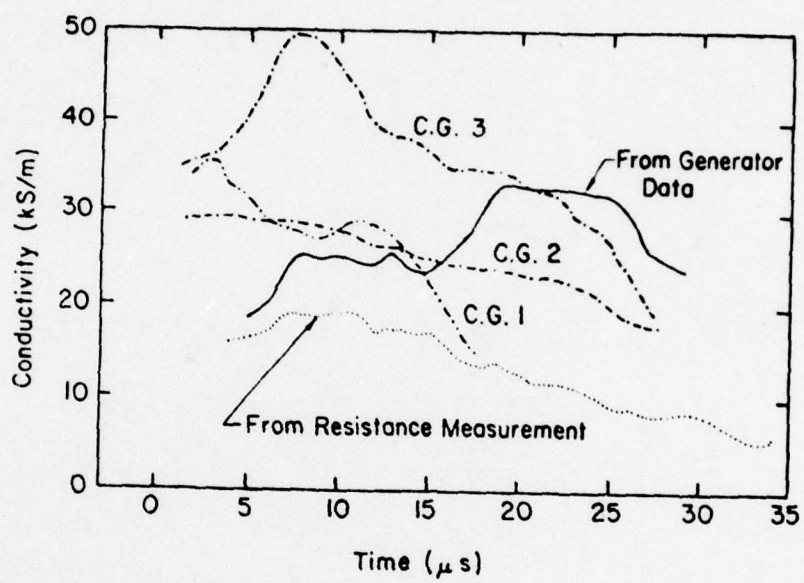
Figure 12 Plasma Conductivity from Various Data Sources (Shot 130-3)

measurements can be determined from Figure 6 and should not be dismissed in accounting for the different conductivity values. The time values shown are from the start of each trace and are at different absolute times. A plot of the values reordered to a laboratory time scale shows some interesting effects. For example, in Figure 13 we note that conductivity appears generally to be increasing as the flow progresses downstream and has a generally decreasing trend with time at a given measurement station.

We also note that the conductivity measurements based on the load measurements and self-excited generator measurements show an increase in conductivity for the first few (< 5) microseconds. If this is a transient effect caused by say, electrode/gas processes, then the agreement in the shape begins to look better. The last maxima in the generator derived trace remains unexplained. As the traces for 130-4 are unreliable late in the flow, no additional data is available for comparison.

We expect that more might be gleaned from this data by an analysis of the various data channels microsecond by microsecond, and propose to use such a technique on future runs.
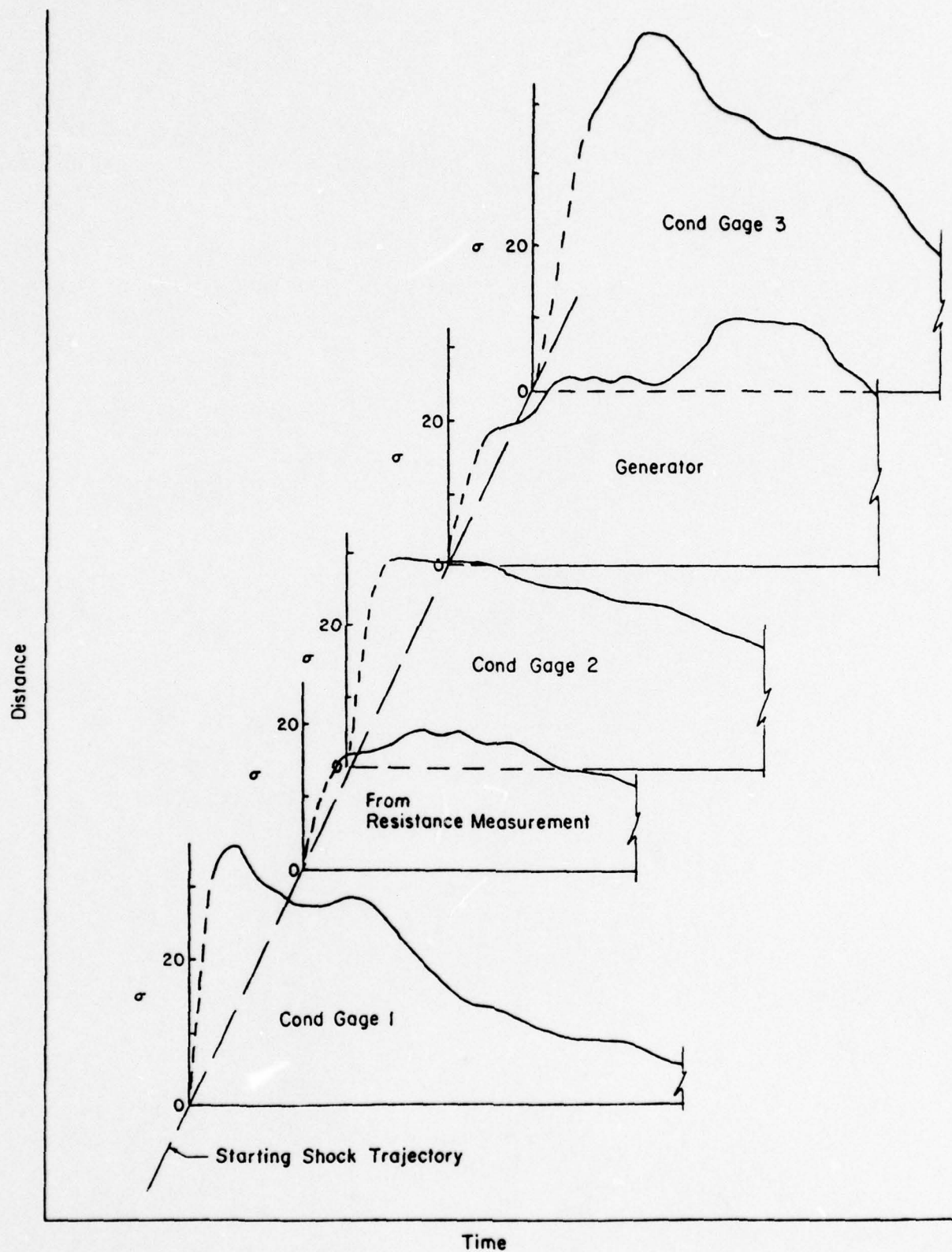
Figure 13 Plasma Conductivity from Various Sources Plotted versus Laborotory Time
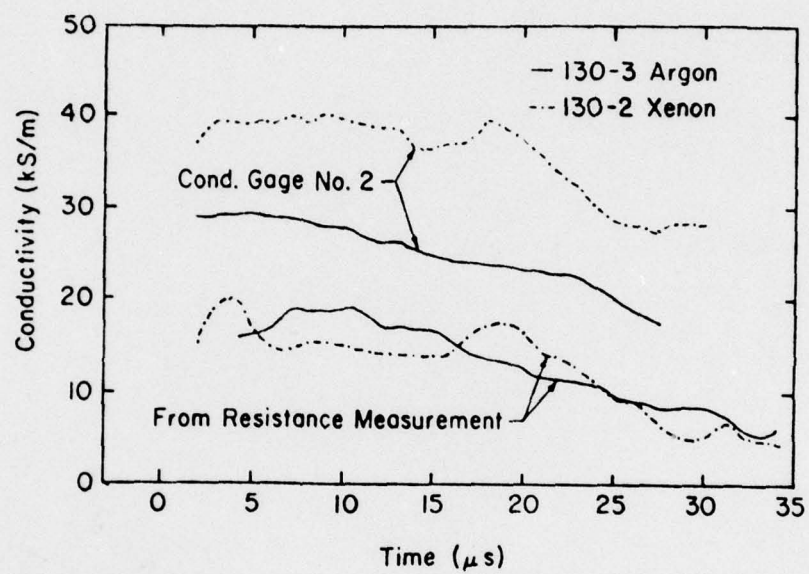
Figure 14 Conductivity Comparison for Xenon and Argon Shots (130-2, 130-3)

A side-by-side comparison of conductivity records
between Shots 130-2 and 130-3 is shown in Figure 14 and
provides another useful result. Conductivity, as measured
by the eddy current conductivity gages, indicate a higher
conductivity for xenon by about 30%. As the average con-
ductivity determined by resistance measurements are com-
parable for the two experiments, this result suggests that
possibly boundary layer effects, which are likely to be
similar in the two cases, are responsible for lowering
average conductivity.

The electrical conductivity histories for Shot 130-4
are shown in Figure 15. The values appear generally correct
but the wide variation at later times suggests instrumenta-
tion problems. The first 10 microseconds for gage 1 appear
reasonable as do the first 7 microseconds of gage 2 and first
5 microseconds of gage 3. Restricting attention to these
times suggests the limited data to be reasonable. Again,
the values obtained from the loaded generator are substan-
tially lower than those measured by the eddy current gages.

3.4 Self-Excited MHD Generator Section

Additionally, Shots 130-3 and 130-4 were run with a
self-excited MHD generator section on each. These diagnostic
devices provide additional information on the flow.
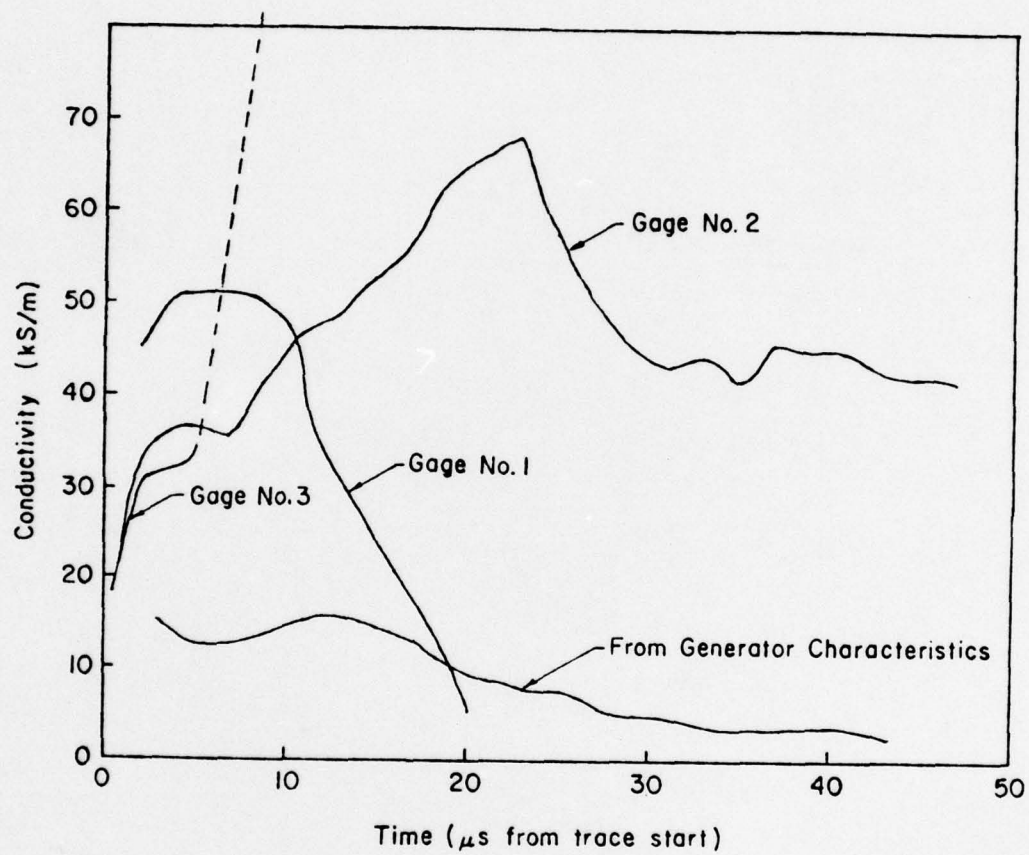
Figure 15 Electrical Conductivity Histories, Shot 130-4

For example, field coil data at the generator station
for 130-3 are shown in Figure 16. Self-excitation is occur-
ring throughout the entire pulse, as evidenced by increasing
current and positive voltage. A short circuit occurs at
34μs, probably due to failure of the Mylar plastic insula-
tion in the coil. Total magnetic field amplification during
the pulse was 19 dB (a factor of 9). Initial increase was
1.3 dB/μs, falling to 0.4 dB/μs at the end of the pulse.

The MHD generator was analyzed for consistency by
using measured plasma parameters to calculate performance,
and then comparing them with observed values. The B-field
magnitude was calculated from measured initial field, current,
and B/I. This was combined with velocity to yield the open
circuit Faraday voltage (Bub) shown in Figure 17.

Initially, at I = 0, the calculated open circuit voltage
exceeds measured field coil voltage. This may be caused by
internal inductance of the generator, forming an inductive
voltage divider with the load. A value of 16 nanohenries
agrees with the data, but is larger than theoretical esti-
mates, which yield about 5 nanohenries. On the other hand,
internal inductance of the load station had previously
been determined to be 14 nanhenries. An alternate explana-
tion is loading of the generator by eddy currents, expected
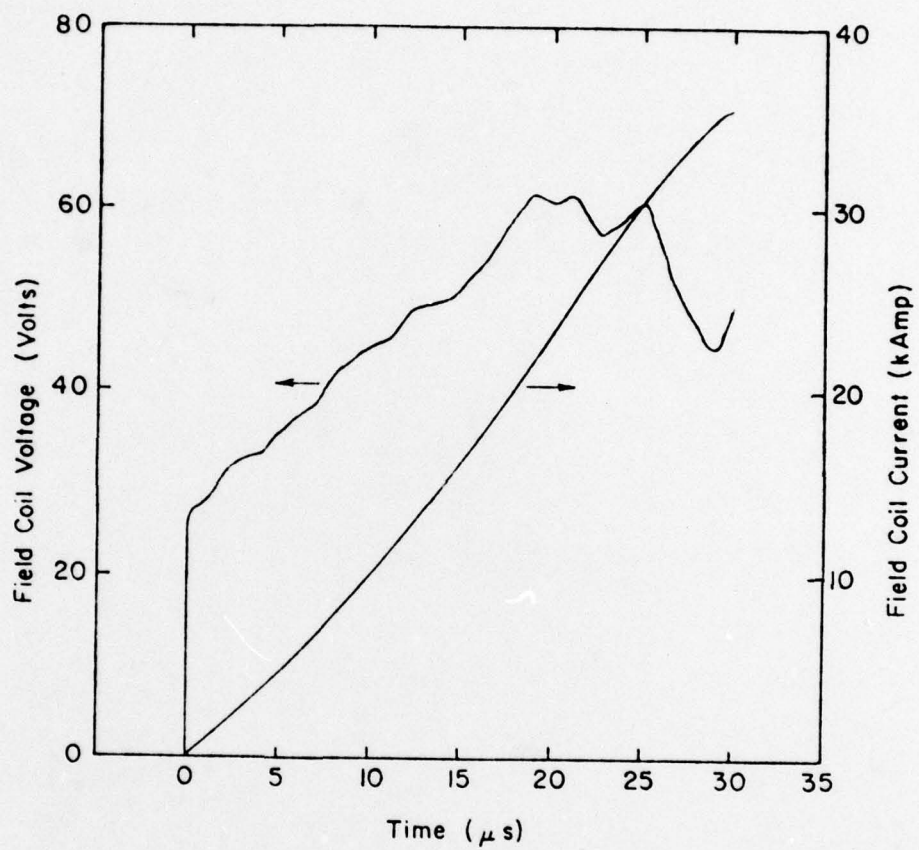
Figure 16 M.H.D. Self-Excited Field Coil
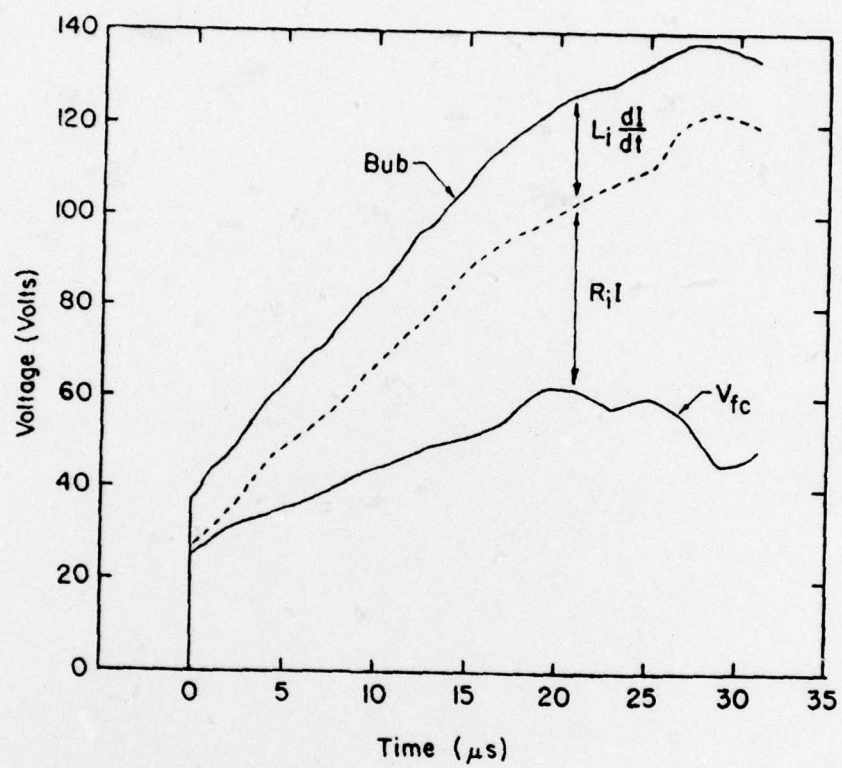
Figure 17 Estimate of Composite Voltage Drops in Generator

because of the very short coil length; this loading would act much like an inductive divider in the present experiment. Some reduction of open circuit Bub was expected, but the observed amount of about 33% appears excessive. Better design of the field coil assembly might well be able to reduce it to 15% or less.

The inductive drop in generator voltage was computed and is also shown in Figure 17. The remaining component of the voltage drop is that due to plasma resistance. By using this voltage drop together with the generator current, plasma resistance and conductivity were determined. The results of this analysis were previously shown together with the other conductivity measurements in Figure 12.

We note that the conductivity estimated from the MHD generator data is consistently higher than the values determined from upstream resistance measurements, and close to free-stream values obtained from eddy current measurements. It should be noted that CG#3 data may be suspect, since fabrication problems caused the shot configuration to differ from the calibration configuration (the coil was closer to the magnet, and the magnets were slightly further apart). Generally the MHD generator data agree reasonably well with the free-stream conductivity values.

The self-excited generator output is shown in Figure 18. Voltages in excess of 85 volts were reached. The observed drop in the voltage at 14 microseconds is probably an instrumentation artifact since its effect is not seen in the instantaneous magnetic field. A peak magnetic field of 0.65 Tesla was reached at 36 microseconds, an increase by a factor of 8.32 over the initial field, or 18.3 dB. This is essentially the same result as was obtained in run 130-3 with a smaller diameter driver.

The measured electrical conductivity determined from the generator characteristics was shown in Figure 15 and is noted to be improved somewhat over 130-3.

3.5 Field Amplification

Figure 19 is a plot of the self-excited field amplification of Shots 130-3 and 130-4. We note from the figure that the 50 percent longer time of the flow of 130-4 did not permit greater field amplification as the trajectory in field-time space is essentially the same as 130-3 with the exception that the absolute values of 130-4 are approximately 10% less than 130-3 at any given time.

The conclusion of this plot is, that longer test times by themselves will not increase field amplification significantly
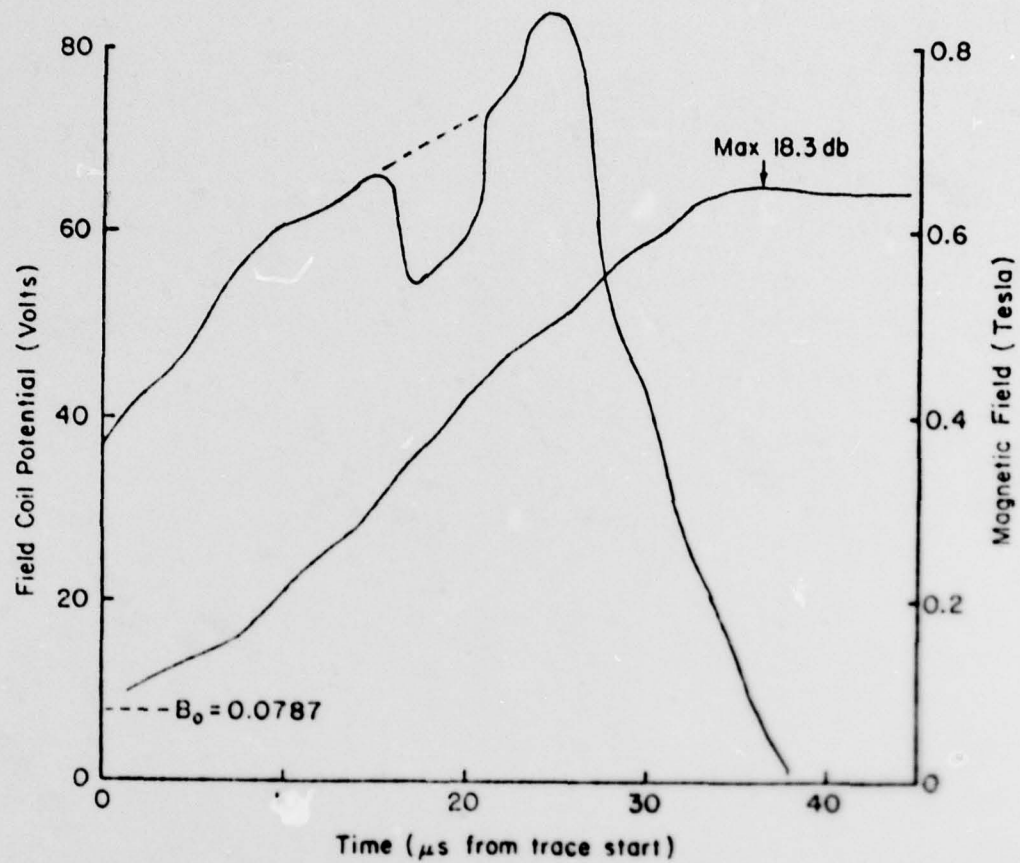
Figure 18 Self Excited Generator Potential and Field vs Time, Shot 130-4
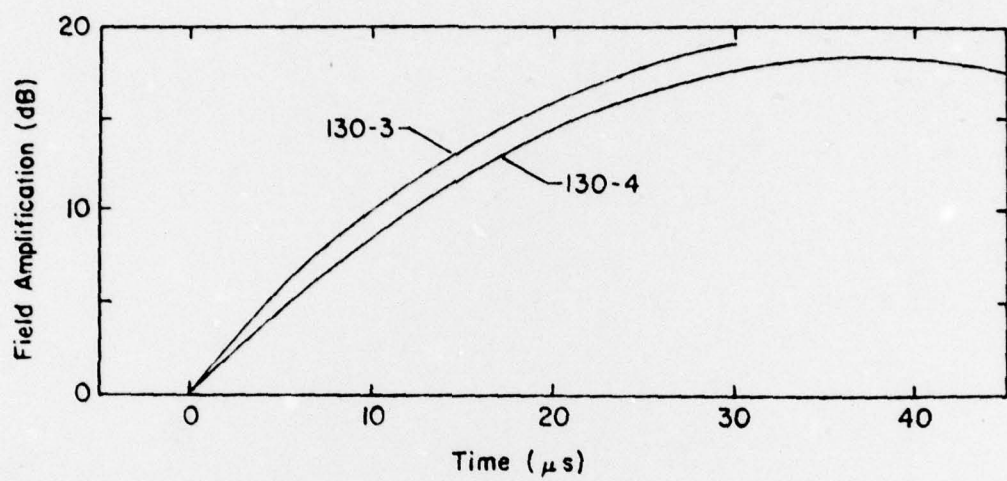
Figure 19 Comparison of Self-Excited Field Amplification

unless the rate of field amplification for early times in the flow are also improved. For example, if the initial enhancement rate of 130-3 of 1.3 dB/μsec could be maintained for 30 microseconds or greater, then a 40 dB improvement (factor of 10^2) increase in magnetic field could be achieved. For the present conditions the field amplification peaks out at 30 to 40 microseconds and the greater test time is not utilized to advantage. This demonstrates that future field enhancement gains must be obtained by simultaneously increasing flow velocity, conductivity and flow duration.

3.6 Summary of Conclusions

This new explosive plasma source can be distinguished from most other high-performance explosive devices, for example the disc driver or the Voitenko compressor, in that the geometry employed in the present device permits a far greater fraction of the gas tube processed initially by a single strong shock. In this way a higher average enthalpy plasma is obtained with the result that one obtains a higher conductivity ($\sigma \sim 38$ kS/m), and the conductivity remains high for a comparatively long period of time in the flow (>20μs).

The flow velocity-history of this plasma source was essentially identical when xenon was replaced by argon.

Bulk electrical conductivity of the argon was about 70%
of the xenon values, and average values from resistance
measurements, about the same.

The self-excited MHD generator worked well, and per-
formed in accordance with theory based on measured field
coil and plasma parameters. A maximum total gain of 19 dB
was accomplished.

The measured electrical conductivities of the larger
source are noted to be improved somewhat over the smaller,
confirming that greater conductivities are possible using
the larger diameter plasma source.

The evidence supports the premise that higher velocity
flow in the channel can also be obtained by the larger dia-
meter source, but that the higher reservoir conditions may
also cause a "pinching off" of the channel entrance and a
premature reduction of flow conditions.

This last effect may be ameliorated by simple geometry
changes near the reservoir to channel transition and will
be addressed in future experiments.

4.   RECOMMENDATIONS

The progress and results of the four experiments designed, fired and analyzed in this period were very satisfying and suggest additional fruitful research.

We recommend a detailed analysis of the time history of the plasma source reservoir conditions including the effect of piston trajectory be made. We feel that by understanding the dynamics of this region we may well be able to tailor the reservoir dynamics to yield optimum conditions in the reservoir and hence downstream in the diagnostic channel.

Additionally, the premature closing of the diagnostic channel entrance, which was uncovered in the present work, may well have been a factor in all of the annular driver runs to date, both smaller driver diameter and large driver diameter. Amelioration of this effect may produce significant gains and should be investigated.

We recommend investigating a plasma source loaded with air, as the driver gas, as preliminary estimates suggest that the electrical conductivity of air at these very high densities may well be similar to that measured using argon and xenon. An experiment such as this confirming this hypothesis would be of interest to and have ramifications for other scientific areas of interest to the Navy.

We recommend investigating different configurations of conductivity gages to resolve the wide variation in measured conductivity, i.e. to determine if the variation is due to the variation of plasma properties with position in the channel or to experimental resolution, and a detailed comparison of the conductivity time histories for clues as to the details of the complex behavior of the flow.

And finally, we recommend additional effort to refine the self-excited generator diagnostic section including modeling of the output, in order to resolve the self-excited generator performance limit problem.

REFERENCES

1. Baum, Dennis W. et al, "Research on Nonideal Plasmas,"
   Artec Associates Incorporated, Final Report 126, Navy
   Contract NR099-414/05-05-77 (473), May, 1978.

2. Gill, Stephen P. et al, "Explosive MHD Research,"
   Artec Associates Incorporated, Annual Report 119,
   Navy Contract N00014-75-C-0822, April, 1976.

3. Baum, Dennis W. et al, "Development of High Energy
   Density Simulator," Artec Associates Incorporated,
   Final Report 120, Defense Nuclear Agency Contract
   DNA001-75-C-0271, December, 1976.

4. Mukherjee, D., "Nonideal Effects in Dense Argon and
   Xenon Plasmas," Proceedings of First ONR Nonideal
   Plasma Workshop, Pasadena, California, 14-15 November,
   1978.

5. Kury, J. W. et al, "Metal Acceleration by Chemical
   Explosives," Fourth Symposium on Detonation, ONR, 1965.

6. Lee, E. et al, "JWL Equation of State Coefficients for
   High Explosives," University of California Lawrence
   Livermore Laboratory, UCID-16189, January, 1973.

7. Flagg, R. F., "A Theoretical Analysis of the Driver-
   Reservoir Method of Driving Hypersonic Shock Tunnels,"
   Proceedings of the Fifth Shock Tube Symposium, USNOL
   28-30 April, 1965.

8. Brown, P. S. et al, "Computational Studies of a Voitenko
   Compressor," University of California Lawrence Livermore
   Laboratory, UCRL-82010, November, 1978.

DISTRIBUTION LIST

Office of Naval Research
Power Program, Code 473
Arlington, Virginia 22217
Attn: J. A. Satkowski   3

Director,
Naval Research Laboratory
Washington, D.C. 20375
Attn: Code 2627   6

Defense Documentation Center
Building 5, Cameron Station
Alexandria, Virginia 22314   12

Office of Naval Research Branch Office
1030 East Green Street
Pasadena, California 91106
Attn: E. T. Florance   1

University of Colorado
Joint Institute for Laboratory Astrophysics
Boulder, Colorado 80309
Attn: Dr. Arthur V. Phelps   1

Naval Surface Weapons Center
Dahlgren, Virginia 22448
Attn: Dr. Frank Rose, Code OF-12   1

NASA Ames Research Center
Moffett Field, California 94035
Attn: Mr. Robert Dannenburg   1

Director,
Naval Research Laboratory
Plasma Physics Division, Code 7770
Washington, D.C. 20375
Attn: Peter J. Turchi   1

Army Corps of Engineers
P.O. Box 1600
Huntsville, Alabama 35807
Attn: Franklin R. Smith, Code ED-FR

STD Corporation
P.O. Box C
Arcadia, California 91006
Attn: Dr. David Oliver   1
       Mr. Clint Bangerter   1

University of Florida
Department of Nuclear Engineering Sciences
Gainesville, Florida   32601
Attn: Prof. R. T. Schneider   1

University of Florida
Department of Engineering Sciences
Gainesville, Florida   32601
Attn: Prof. Horst Wilhelm   1

Headquarters
Defense Nuclear Agency
Washington, D.C.   20305
Attn: John Farber   1

University of Nevada
Desert Research Institute System
Reno, Nevada 89507
Attn: Prof. S. Winterberg   1

Artec Associates Inc.
26046 Eden Landing Road
Hayward, California 94545
Attn: Dr. Dennis W. Baum   1
       Dr. Stephen P. Gill   1
       Dr. Deb Mukherjee   1
       Dr. Robert F. Flagg   1

General Electric Company
Manager, MHD Programs
Valley Force Space Center
P.O. Box 8555
Philadelphia, Pennsylvania   19101
Attn: Dr. Bert Zauderer   1

University of Arizona
Head, Department of Planetary Sciences
Tucson, Arizona 85721
Attn: Prof. W. B. Hubbard   1

```
Lawrence Livermore Laboratory
H - Division
Livermore, California  94550
Attn:  Dr. Hugh E. Dewitt                        1
       Dr. F. J. Rogers                          1
       Dr. Harold Grabowski                      1
       Dr. Marvin Ross                           1
       Dr. Richard More                          1


University of Rochester
Laboratory for Laswer Energetics
215 East River Road
Rochester, New York  14627
Attn:  Dr. Robert McCrory                        1
       Dr. Stanley Skupsky                       1


Los Alamos Scientific Laboratory
Los Alamos, New Mexico  87545
Attn:  Dr. Robert Malone                         1
       Dr. Ping Lee                              1
       Dr. John Shanner                          1
       Dr. Walter Huebner                        1
       Dr. Donald Dubois                         1
       Dr. Max Fowler                            1


University of Missouri
Physics Department
Rolla, Missouri  65401
Attn:  Prof. K. Nygaard                          1
```